

1 **Precipitation stable isotopic signatures of tropical cyclones in Metropolitan**
2 **Manila, Philippines show significant negative isotopic excursions**

4 Dominik Jackisch¹, Bi Xuan Yeo², Adam D. Switzer^{1,2}, Shaoneng He¹, Danica Linda M.
5 Cantarero³, Fernando P. Siringan³ and Nathalie F. Goodkin^{1,2,4}

7 ¹Earth Observatory of Singapore, Nanyang Technological University, Singapore

8 639798

9 ² Asian School of the Environment, Nanyang Technological University, Singapore

10 639798

11 ³ Marine Science Institute, University of the Philippines Diliman, Quezon City 1101,
12 Philippines

13 ⁴ American Museum of Natural History, New York 10024, USA

15 Correspondence to: Adam D. Switzer (aswitzer@ntu.edu.sg)

17 **Abstract**

19 Tropical cyclones have devastating impacts on the environment, economies, and societies,
20 and may intensify in the coming decades due to climate change. Stable water isotopes serve
21 as tracers of the hydrological cycle, as the fractionation process may leave distinct
22 precipitation isotopic signatures. Here we present a record of daily precipitation isotope
23 measurements from March 2014 to October 2015 for Metropolitan Manila, which is a first of
24 a kind dataset for the Philippines and Southeast Asia, and analyze the isotopic variation
25 related to tropical cyclones. The most negative shift in $\delta^{18}\text{O}$ value (-13.84 ‰) leading to a
26 clear isotopic signal was caused by Typhoon Rammasun, which directly hit Metropolitan
27 Manila. The average $\delta^{18}\text{O}$ value of precipitation associated with tropical cyclones is -10.24 ‰,
28 whereas the mean isotopic value for rainfall associated with non-cyclone events is -5.29 ‰.
29 Further, the closer the storm track to the sampling site, the more negative the isotopic values,
30 indicating that in-situ isotope measurements can provide a direct linkage between isotopes
31 and typhoon activities in the Philippines.

32 **1. Introduction**

33

34 The Philippine archipelago, with its fast-growing population clustered along the coastline, is
35 one of the most vulnerable countries to climate change (Cinco et al., 2014). It is especially
36 prone to the devastating effects of tropical cyclones. Thus, it is considered a hotspot region
37 for hydrometeorological disasters (Cinco et al., 2014; Cruz et al., 2013; Takagi and Esteban,
38 2016). There is a clear need for developing a better understanding of tropical cyclone (TC)
39 dynamics and cyclone histories in the context of prediction that may allow government
40 agencies to implement proper mitigation and adaptation policies. Nine TCs per year made
41 landfall on average between 1951 to 2013 in the Philippines. The number of TCs not making
42 landfall but reaching Philippine waters is substantially higher with 19.4 per year (Cinco et al.,
43 2016). Changing climate and associated warming of the surface ocean, will likely increase the
44 intensity of tropical cyclones in the future (Emanuel, 2005; Webster and Holland, 2005;
45 Woodruff et al., 2013).

46

47 The Philippines were struck by several devastating TCs in recent years (Table 1). Typhoon
48 Haiyan (2013) which tracked over the Visayas has been the costliest TC to date (~ 2.06 billion
49 USD in 2013), with strong winds and intense storm surges inundating coastal areas resulting
50 in more than 6000 fatalities (Alojado and Padua, 2015; Lagmay et al., 2015; Soria et al., 2016).
51 Typhoon Rammasun, which made landfall in July 2014, is ranked number 3 with ~ 880 million
52 USD in 2014 (Alojado and Padua, 2015; NDRRMC, 2014). Eighty percent of the strongest
53 typhoons making landfall in the Philippines over the last three decades developed during
54 higher than average sea surface temperatures (SST), which supports evidence that TC
55 intensities are projected to rise in the future due to an increase in global temperatures (Guan
56 et al., 2018; Webster and Holland, 2005; Takagi and Esteban, 2016). For example, SST was
57 found to be anomalously high and reaching 29.6 °C during the formation of Typhoon Haiyan
58 (Takagi and Esteban, 2016). The average Philippines' ocean SST we have calculated for the
59 period 1945 to 2014 (basin between 6° – 18° N, 120° – 140° E) is ~ 28.5 °C based on National
60 Oceanic and Atmospheric Administration Extended Reconstructed Sea Surface Temperature
61 Dataset, Version 5 (NOAA ERSST v5) (Takagi and Esteban, 2016). By the end of the 21st
62 century, average typhoon intensity in the low-latitude northwestern Pacific is predicted to
63 increase by 14 % due to warming ocean temperatures (Mei et al., 2015).

64

65 A few studies have demonstrated the potential to investigate tropical cyclones using stable
66 water isotopes (Good et al., 2014; Lawrence et al., 2002; Munksgaard et al., 2015; Pape et al.,
67 2010). Stable water isotopes ($\delta^2\text{H}$ and $\delta^{18}\text{O}$) serve as dynamic tracers of hydrological
68 processes and can provide insights into the water and energy budgets of TCs (Good et al.,
69 2014; Lawrence and Gedzelman, 1996). For regions with general TC occurrence, significantly
70 lower $\delta^2\text{H}$ and $\delta^{18}\text{O}$ are associated with TC rainfall due to strong fractionation processes,
71 compared to other tropical rain events (Lawrence, 1998; Lawrence and Gedzelman, 1996).
72 Furthermore, $\delta^2\text{H}$ and $\delta^{18}\text{O}$ have been used successfully to interpret TC history from
73 paleoarchives, such as tree rings and speleothems (Oliva et al., 2017). For instance, tree-ring
74 cellulose isotope proxies have recorded the recent 220 years of cyclones in the southeastern
75 USA (Miller et al., 2006); similarly, high-resolution isotopic analysis of tree-rings from the
76 eastern US revealed the occurrence of hurricanes in 2004 (Li et al., 2011); a 23-year stalagmite
77 record from Central America was used to reconstruct past TC activity (Frappier et al., 2007),
78 and isotope signals from a 800-year stalagmite record were used to reconstruct past TC
79 frequencies in northeastern Australia (Nott et al., 2007). Interpretation of TC history in
80 paleotempestology from paleoarchives is based on the fact that TCs leave distinct isotopic
81 signatures on precipitation, possibly providing information on TC's evolution and structure
82 (Lawrence et al., 2002).

83

84 The depletion in isotopes is attributed to the high condensation levels, strong isotopic
85 exchanges between inflowing water vapour and falling raindrops in cyclonic rainfall bands,
86 resulting in a temporal decrease of isotopic values throughout a rain event (i.e. amount effect)
87 (Lawrence, 1998; Lawrence and Gedzelman, 1996). Isotopic depletion is further enhanced by
88 TC's thick, deep clouds, relatively large storm size and longevity (Lawrence, 1998).
89 Furthermore, while isotopic depletion increases inwards towards the eye wall of the storm
90 (Lawrence and Gedzelman, 1996), isotope ratios inside the inner eye wall region are relatively
91 enriched, likely due to an intensive isotopic moisture recharge with heavy isotopes from sea
92 spray (Fudeyasu et al., 2008; Gedzelman et al., 2003). These findings are based on work
93 conducted in the 1990s in Puerto Rico and on the southern and eastern coasts of the United
94 States. More recently, these previous findings have been confirmed by studying TCs which
95 occurred in a few other regions, such as in China or Australia (Chakraborty et al., 2016;

96 Fudeyasu et al., 2008; Good et al., 2014; Munksgaard et al., 2015; Xu et al., 2019).

97

98 The above-mentioned studies are geographically limited to a few locations globally, with no
99 studies in Southeast Asia and the Philippines in particular. In this manuscript, we present the
100 first such study for the Philippines, with daily isotope measurements of precipitation from
101 Metropolitan Manila (the National Capital Region) spanning from March 2014 to October
102 2015. During the study period, nine tropical cyclones passed by or made landfall within 500
103 km of the sampling site (Fig. 1). The major objective of this research is the following:

- 104 - To understand if there is an isotopic variation in precipitation associated to the TC
105 landfall in the Philippines and if tropical cyclones leave clear isotopic signals.
- 106 - To identify the isotopic signals measured for Metropolitan Manila and the intensity of
107 the isotopic depletion associated to TC activities, and to identify how it is represented
108 spatially.
- 109 - To understand the isotopic variation with distance from the TC track in the Philippines.

110 Our findings provide a baseline dataset for reconstruction of typhoon activities using stable
111 isotopes and contribute to a better understanding of past and future TC activities in the
112 Philippines.

113

114

115 **2. Materials and methods**

116

117 **2.1 Site description**

118

119 The Philippines is a Southeast Asian country comprising more than 7000 islands located in the
120 Northwest Pacific between 4° 40' N and 21° 10' N, and 116° 40' E and 126° 34' E (Fig. 1). The
121 country experiences an average annual rainfall of about 2000 mm, influenced by two
122 monsoon seasons, the northeast monsoon from November to April and the southwest
123 monsoon from May to October (Cinco et al., 2014). About 35 % of the annual rainfall is related
124 to TC activity, while that number rises to about 50 % for Luzon and decreases to 4 % for the
125 southern island of Mindanao (Cinco et al., 2016). Part of the rainfall amount in the Philippines
126 is of orographic nature due to north-south oriented mountain ranges of more than 1000 m
127 spanning the largest islands of Luzon and Mindanao (Villafuerte et al., 2014). The majority of

128 the steadily growing population in the Philippines (101 million 2017 census) live in densely
129 populated, low-elevation areas close to the coastlines (Cinco et al., 2014, 2016; Philippine
130 Statistics Authority, 2017).

131

132

133 **2.2 Isotopic data**

134

135 In total, 186 daily precipitation samples were collected from 10 March 2014 to 26 October
136 2015 using a PALMEX collector (Gröning et al., 2012) at the Marine Science Institute of the
137 University of the Philippines Diliman located in Quezon City, which is part of Metropolitan
138 Manila. The rain collection station was installed on the rooftop of the Marine Science Institute
139 (14°39'02.5"N, 121°04'08.6"E), which is centrally situated in the campus and surrounded by
140 trees and various green spaces. The rooftop location proved ideal for rainwater collection as
141 it allowed for unobstructed access to rainwater without any potential sources of
142 contamination. Samples were collected daily at 10 am, and transferred without headspace to
143 30-ml HDPE bottles made by AZLON for storage prior to analysis. Samples were sent to the
144 Earth Observatory of Singapore, Nanyang Technological University, Singapore and were
145 analyzed for stable isotopes using a Picarro L1240-i laser spectroscopy instrument. We
146 followed the procedures described by Van Geldern and Barth (2012) for post-run corrections
147 and calibration. Three in-house water standards used for calibration include KONA (0.02 ‰
148 of $\delta^{18}\text{O}$; 0.25 ‰ of $\delta^2\text{H}$), TIBET (-19.11 ‰ of $\delta^{18}\text{O}$; -143.60 ‰ of $\delta^2\text{H}$), and ELGA (-4.25 ‰ of
149 $\delta^{18}\text{O}$; -27.16 ‰ of $\delta^2\text{H}$). They are calibrated against the international reference water
150 VSMOW2 and SLAP2. Long-term analysis of our QA/QC standards yields precision of 0.04 ‰
151 for $\delta^{18}\text{O}$ and 0.2 ‰ for $\delta^2\text{H}$.

152

153 **2.3 Cyclone track data**

154

155 The International Best Track Archive for Climate Stewardship (IBTrACS) dataset contains
156 global TC best-track data, and is a joint effort of various regional meteorological institutions
157 and centers that are part of the World Meteorological Organization (WMO). The data is
158 publicly available, and comprises information on storm eye/center with its coordinates, wind
159 speed, and pressure, etc., with a temporal resolution of six hours (Knapp et al., 2010; Rios

160 Gaona et al., 2018). Apart from visualization of cyclone paths, we used the dataset to calculate
161 the spatial distance between the storm's eye coordinates and our sampling site.

162

163 **2.4 Satellite precipitation data**

164

165 We used the IMERG Version 5 Final daily product, a remotely-sensed precipitation dataset
166 from satellites to highlight cyclonic tracks and precipitation patterns of several TC's passing
167 by Metropolitan Manila, and to identify which rainfall events were not affected by cyclonic
168 activity, and instead were associated with local or other regional convection activities. Such
169 datasets are beneficial as they provide quasi-global grid-based rainfall estimates for land and
170 the oceans (Poméon et al., 2017). The Integrated Multi Satellite Retrievals for GPM (IMERG)
171 from the Global Precipitation Measurement (GPM) programme with a fine 0.1-degree grid
172 size (Huffman et al., 2017) has been available since March 2014, and provides precipitation
173 data in different temporal resolutions, such as half-hourly or daily. Such satellite rainfall data
174 has been previously utilized to show TC tracks and related rainfall intensities (Rios Gaona et
175 al., 2018; Villarini et al., 2011).

176

177 **2.5 Rainfall, temperature and relative humidity data**

178

179 Daily rainfall, mean daily relative humidity and mean daily temperature data was obtained
180 from the Philippine Atmospheric, Geophysical and Astronomical Services Administration
181 (PAGASA), which maintains a rainfall monitoring station about 2.7 km away from our sampling
182 site. The data is freely available for the period 2013 to 2017, and can be accessed on the
183 Philippines Freedom of Information website (www.foi.gov.ph).

184

185

186 **3. Results**

187 **3.1 Isotopic variation of stable isotopes in precipitation**

188

189 The stable isotope composition during the 19 months study period spanning from 10 March
190 2014 to 27 October 2015 shows large seasonal isotopic variability in Metropolitan Manila.
191 One hundred and eighty-six daily precipitation samples have been collected and analyzed in

192 total (Fig. 2). $\delta^{18}\text{O}$ ranges from 4 ‰ to -13.84 ‰, and $\delta^2\text{H}$ from 16.84 ‰ to -99.1 ‰. The
193 highest $\delta^{18}\text{O}$ value of 4 ‰ was observed on 9 April 2014 during the annual dry period, whereas
194 the lowest $\delta^{18}\text{O}$ value of -13.84 ‰ was observed on 16 September 2014 in association with
195 TC activity. The mean $\delta^{18}\text{O}$ of precipitation at the study site is -5.29 ‰ for non-TC rain systems,
196 while TCs, as large regional convective systems, have the potential to cause a change in δ -
197 values of up to almost 9 ‰ relative to the mean. The average $\delta^{18}\text{O}$ value of the nine TCs that
198 tracked within <500 km from the sampling site is -10.24 ‰ (STDEV of 2.11), a factor of 2 larger
199 than the mean from non-TC precipitation (average is -5.29 ‰, STDEV of 2.64).

200

201 An inter-annual variation of stable isotopes in precipitation is observed in the time series of
202 Metropolitan Manila, where the generally rainfall intensive and humid summer months
203 exhibit lower isotope values compared to the rest of the year (Fig. 2). The precipitation
204 isotopes are characterized by slightly higher values during winter and spring, when
205 temperatures and relative humidity are lower and rainfall is less frequent. Especially early
206 2015 shows drier conditions with sporadic rainfall and relative humidity levels of about 60 %
207 to 70 %. This is also reflected in $\delta^{18}\text{O}$ and $\delta^2\text{H}$ for instance on 1 March 2015 with 0.01 ‰ and
208 9.8 ‰ respectively. Deuterium excess, which is defined as $d\text{-excess} = \delta^2\text{H} - 8 * \delta^{18}\text{O}$, is
209 commonly regarded to reflect evaporation conditions of moisture source regions. In contrast
210 to the other parameters, $d\text{-excess}$ shows less variability throughout the time series and
211 mainly clusters in a relatively small range of 5 ‰ to 15 ‰. To be precise, the $d\text{-excess}$ values
212 range from -15.18 ‰ to 24.31 ‰.

213

214 Based on the daily isotope measurements of rainfall events between 2014 and 2015, we
215 determined the LMWL (local meteoric water line) for the study site as $\delta^2\text{H} = 7.2674 \times \delta^{18}\text{O} +$
216 5.4103 (Fig. 3), indicating that slope and intercept of the LMWL are lower due to the influence
217 of tropical precipitation compared to the GMWL (global meteoric water line) with $\delta^2\text{H} = 8 \times$
218 $\delta^{18}\text{O} + 10$ (Craig, 1961).

219

220 In order to assess meteorological controls on the isotopic composition of daily precipitation
221 at Metropolitan Manila, we investigated the correlation between $\delta^{18}\text{O}$, daily precipitation
222 amount, daily mean temperature and daily mean relative humidity. Additionally, $\delta^{18}\text{O}$ is
223 compared to $d\text{-excess}$ ($n=187$) (Fig. 4). A weak correlation was found between $\delta^{18}\text{O}$ and d -

224 excess ($R^2=0.2187$) and between $\delta^{18}\text{O}$ with precipitation amount ($R^2=0.1087$) and between
225 $\delta^{18}\text{O}$ with relative humidity ($R^2=0.1323$). There is no association between $\delta^{18}\text{O}$ and
226 temperature ($R^2=0.0338$).

227

228 In order to get further insights into the seasonal variations, we also calculated the average
229 values for each month in the time series for every isotopic and climatic parameter (Table 2).
230 $\delta^{18}\text{O}$ is relatively low during the summer months, for instance with -7.29 ‰ in September
231 2014 compared to the months of winter and spring with -0.53 ‰ in April 2014 or -0.66 ‰ in
232 February 2015. Similarly, the average monthly rainfall is less in winter and spring with 4.3 mm
233 in March 2014 and 5.8 mm in January 2015 compared to the summer months such as July and
234 August 2014 with 19 mm and 20 mm respectively. As mentioned before regarding the daily
235 measurements, we also observe on the monthly scale conditions which are more humid in
236 the summer. We calculated the correlation to investigate the relationship between the
237 isotopic composition of precipitation ($\delta^{18}\text{O}$) with meteorological parameters (average
238 monthly rainfall, relative humidity and temperature) on a monthly scale. $\delta^{18}\text{O}$ and $\delta^2\text{H}$ are
239 strongly correlated with $r=0.96$ ($n=18$, $p\text{-value}=<0.0001$ and 99% confidence level), whereas
240 the relationship between $\delta^{18}\text{O}$ and d-excess yields an r of -0.64 ($n=18$, $p\text{-value}=0.003$). A
241 negative correlation was clearly determined between $\delta^{18}\text{O}$ and precipitation with $r=-0.77$
242 ($n=18$, $p\text{-value}=0.0002$) and between $\delta^{18}\text{O}$ and relative humidity with $r=-0.85$ ($n=18$, $p\text{-value}=<0.0001$). $\delta^{18}\text{O}$ and temperature are not correlated with $r=0.04$ ($n=18$, $p\text{-value}=0.87$).

244

245 **3.2 Precipitation isotope evolution during TC events**

246

247 Overall, precipitation isotopes associated with TCs mark the lower range of $\delta^{18}\text{O}$ values during
248 the study period. Especially during the 2014 season, most of the very low precipitation
249 isotope values occurred throughout passage of TCs. For instance, Rammasun led to the lowest
250 δ -value (Fig. 5, point a, -13.84 ‰) of the whole study period, while other TCs such as Fung-
251 Wong (Fig. 5, point c, -12.16 ‰), Kalmaegi (Fig. 5, point b, -11.39 ‰), or Hagupit (Fig. 5, point
252 d, -9.88 ‰) caused other negative excursions in isotopic values. The 2015 season is
253 characterized by on average a slightly higher isotopic enrichment during the rainfall intensive
254 summer months. Nonetheless, a similar noticeable isotope signal is visible with low $\delta^{18}\text{O}$
255 isotopes, clustered along the lower end of the sample range, for example, caused by Linfa

256 (Fig. 5, point f, -8.5 ‰) or Koppu (Fig. 5, point i, -8.7 ‰). The other TCs that occurred during
257 the study period and were investigated by us were Mekkhala (Fig. 5, point e, -10.77 ‰),
258 Twelve (Fig. 5, point g, -7.7 ‰) and Mujigae (Fig. 5, point h, -7.5 ‰). However, relatively
259 negative isotope samples (Fig. 5) also originated from non-TC rainfall systems. Those events
260 are discussed below.

261

262 Out of the nine TCs that occurred within a 500 km radius from the sampling site, Rammasun
263 and Kalmaegi left clearly observable, distinct isotopic signatures during their approach and
264 dissipation, which we will therefore present in more detail in the next paragraphs. Typhoon
265 Hagupit (Fig. 5, point d) similarly lead to a clear isotopic evolution pattern during its time of
266 occurrence in the Philippines and is shown in the supplementary (S1).

267

268 Typhoon Rammasun's rainfall intensities based on the IMERG precipitation data together
269 with its track from IBTrACKS is shown in Fig. 6a. Typhoon Rammasun stands out in our study
270 period as it moved straight towards the National Capital Region of the Philippines, resulting
271 in a direct hit. Rammasun, locally named Glenda, made landfall in the Bicol region of southern
272 Luzon on 15 July, with wind speeds of about 160 km/h. On 16 July, it passed south of
273 Metropolitan Manila 50 km from our sampling site, with maximum winds of 130 km/h,
274 gradually losing strength over land. As Rammasun approached on 15 July, the precipitation
275 has shown relatively high $\delta^{18}\text{O}$ of -4 ‰ while rainfall was weak (Fig. 7a). On 16 July, $\delta^{18}\text{O}$
276 shifted to -13.84 ‰, while the typhoon's track was the closest to our sampling site and rainfall
277 amount was high. As Rammasun moved away, precipitation isotopes became more positive,
278 and rainfall amount decreased. The characteristic isotopic evolution related to Rammasun's
279 distance and rainfall intensities as a function of time can be seen in Fig. 8a, where the different
280 radii indicate the distance to the sampling site, and the strong isotopic depletion observed on
281 16 July is also evident. As Rammasun with its storm center tracked towards the northwest
282 and away from Metropolitan Manila, our precipitation samples were relatively isotopically
283 enriched for the following two days, namely -9.12 ‰ on 17 July and -6.26 ‰ on 18 July.

284

285 Typhoon Kalmaegi, locally named Luis, was the first typhoon to make landfall in the
286 Philippines two months after Rammasun. Kalmaegi reached typhoon intensity on 13
287 September, making landfall the following day in northern Luzon, with maximum wind speeds

288 of about 120 km/h. Kalmaegi tracked relatively far away from the sampling site (about 350
289 km), but the accumulated rainfall it produced was centered south of the track, placing it
290 considerably closer to the National Capital Region (Fig. 6b). Despite the distance of the eye
291 from the sampling site, a characteristic isotopic pattern was visible, with the most negative
292 $\delta^{18}\text{O}$ value of -11.39 ‰ on 15 September, coincident with the highest rainfall (Fig. 7b). The
293 following day, $\delta^{18}\text{O}$ values returned to higher values with the increase in distance from the
294 eye. This is also seen in a spatial representation in Fig. 8b, visualizing the track of Kalmaegi
295 and the respective $\delta^{18}\text{O}$ values. Kalmaegi was first approaching the sampling site on 14
296 September and passed away on 15 and 16 September. The lowest $\delta^{18}\text{O}$ was measured on 15
297 September and is indicated in the figure in dark blue colour.

298

299

300 **4. Discussion**

301 **4.1 Stable isotopes of precipitation – a possible tracer for TCs**

302

303 As stable water isotopes fractionate during the physical process of evaporation and
304 condensation, they serve as effective tracers in the hydrological cycle (Dansgaard, 1964; He
305 et al., 2018; Risi et al., 2008; Tremoy et al., 2014). Here, we have demonstrated that stable
306 water isotopes can possibly be used to identify TC activity in the Southeast Asian region by
307 excursions in $\delta^{18}\text{O}$, providing evidence and supporting the hypothesis that TCs may leave a
308 clear isotopic signal in the Philippines. The strong isotopic depletion is due to high
309 condensation efficiencies in cyclonic convective rain bands, leading to extensive
310 fractionation. This is particularly pronounced in intense, large-scale TCs (Lawrence, 1998;
311 Lawrence and Gedzelman, 1996). In the previous section, we have presented our findings of
312 precipitation isotope ratios associated with typhoon activities affecting Metropolitan Manila
313 during the study period of March 2014 to October 2015. Based on our time series, we
314 therefore argue that for the Philippines, the lowest measured isotope value likely indicates
315 the occurrence of a TC, such as is the case for Typhoon Rammasun (Fig. 5). Similarly, other
316 anomalously low $\delta^{18}\text{O}$ values at our site are caused by TC making landfall or passing by.

317

318 Individual TCs (Rammasun and Kalmaegi) were characterized by consistent isotopic
319 excursions to very negative values in a range of up to -9 ‰ compared to the mean isotopic

320 value of -5.29 ‰ (Fig. 7 and 8). A TC approaching the sampling site had relatively higher
321 isotope values than at its later stages when it was closest to the site in Metropolitan Manila.
322 When at its closest, strong rainfall together with increased fractionation depleted
323 precipitation isotopes, leading to a distinct drop in isotope value. Such a strong negative
324 isotopic shift in precipitation has been previously observed in other regions (Fudeyasu et al.,
325 2008; Lawrence and Gedzelman, 1996; Munksgaard et al., 2015; Xu et al., 2019). As the TC
326 moved away and rainfall intensities weakened, $\delta^{18}\text{O}$ in precipitation became again more
327 positive, likely due to evaporative effects (Munksgaard et al., 2015; Xu et al., 2019).

328

329 As the strongest TC in terms of wind speeds, damage costs, and fatalities, Typhoon Rammasun
330 reduced the isotope values most during our study period, to -13.84 ‰. Similarly, Typhoon
331 Kalmaegi lead to extensive damage and caused a significantly negative excursion in
332 precipitation isotopes to -11.39 ‰, suggesting that the lowest isotope values might indicate
333 the occurrence of the strongest TC at that time at our site in the Philippines. We note that
334 our isotopic measurements are similar to observations elsewhere. For example, the range of
335 $\delta^{18}\text{O}$ values caused by Typhoon Shanshan affecting the subtropical Ishigaki island was -6 to -
336 13 ‰, (Fudeyasu et al., 2008); Tropical Cyclone Ita led to a range of -4.8 to -20.2 ‰ in
337 northeastern Australia (Munksgaard et al., 2015); several TCs which made landfall in Texas
338 resulted in isotope values from -3.9 to -14.3 ‰ (Lawrence and Gedzelman, 1996); or
339 hurricanes that affected Puerto Rico and southern Texas were found to deplete $\delta^{18}\text{O}$ up to -
340 18 ‰ (Lawrence, 1998). The lowest value resulting from Typhoon Phailin on the Andaman
341 Islands was reported to be -5.5 ‰, and Typhoon Lehar depleted the precipitation sample to
342 -17.1 ‰ (Chakraborty et al., 2016). For TCs within a distance of up to 500 km from the
343 sampling site at the University of the Philippines Diliman in Metropolitan Manila we measured
344 an isotopic range of -7.7 ‰ (Typhoon Koppu) to -13.84 ‰ (Typhoon Rammasun). Despite the
345 overall comparability to our measurements, differences exist. The lowest values observed in
346 some studies are considerably more negative than at our site (Lawrence, 1998; Munksgaard
347 et al., 2015). However, we attribute these differences to a variety of features, such as the
348 specific climatic condition at each site, differences in temperature, humidity, and altitude or
349 latitude, which are likely contributing factors to the observed isotopic variation by altering
350 isotopic fractionation. Further, rainout history, location of typhoon tracks, topography,
351 respective strength of each TC, as well as its distance to the sampling site most likely have a

352 significant influence as well (Fudeyasu et al., 2008; Good et al., 2014; Munksgaard et al., 2015;
353 Xu et al., 2019).

354

355 In order to assess why other very low isotopic excursions occurred on various days (Fig. 5) we
356 used IMERG satellite precipitation data. IMERG data with its fine spatio-temporal resolution
357 allows the identification of convective rainfall areas and the passage of TCs and other rain
358 systems (Fig. 6). Our analysis shows that precipitation events with anomalously low isotope
359 signals unassociated with TCs are largely related to local, strong convective rainfall events or
360 large scale and slow-moving rain areas passing over the National Capital Region. Therefore,
361 the degree of convection is responsible to produce the other observed low $\delta^{18}\text{O}$ value outliers
362 that are not related to cyclone rainfall, as strong convection and long stratiform rainfall leads
363 to intense fractionation (He et al., 2018; Risi et al., 2008; Tremoy et al., 2014). Contrarily, we
364 speculate that the more positive isotope values which cluster along the higher end of the
365 sample spectrum around 0 ‰, are associated with local, short convective rainfall events and
366 light intensity rain as confirmed with IMERG satellite precipitation data. Additionally, the
367 PAGASA rain gauge data indicates that rainfall amounts are very low during days with such
368 very enriched isotope samples, such as 0.3 mm/day for the highest recorded sample of 4 ‰
369 on 9 April 2014. Interestingly, TCs at our site were found to be related with low isotope values
370 together with high rainfall amounts (Fig. 5), while the majority of other low isotopic values
371 unassociated with TCs were characterized by on average lesser rainfall amounts. This possibly
372 indicates that TCs in the Philippines, besides using for instance modern-day satellite or radar
373 data, can be detected using these two parameters, i.e. strong isotopic depletion coupled with
374 high rainfall amounts.

375

376 The aforementioned local convective precipitation events have the potential to induce a
377 signal of very negative $\delta^{18}\text{O}$ values which are not related to TC activities. We therefore label
378 such a signal as a “false non-TC signal”, as it is induced by non-TC rainfall. This results in the
379 fact that TCs occurring during our study period do not entirely cluster along the lowest range
380 of isotope values as seen in figure Fig. 5. Nevertheless, Typhoon Rammasun caused a clear
381 drop in isotopes and stands out in the dataset. This might be the case because Rammasun’s
382 track and heavy rainfall comes in closest proximity (50 km) to the sampling site. Other TCs
383 occurring within the 500 km radius did not lead to such a clear negative isotopic signature,

likely because these typhoons did not pass the sampling site at all or heavy rainfall occurred elsewhere within the TC rainfall system (see S 2 for their tracks and accumulated rainfall areas). Some of these TCs have intense rainfall areas over other parts of the Philippines and are characterized by a variable track, likely influenced by land interactions. Land interaction reduces TC strength and can lead to rain out due to orographic effects induced by the north-south oriented mountain ranges (Park et al., 2017; Xie and Zhang, 2012; Xu et al., 2019). Especially Typhoon Koppu rained out before making landfall and abruptly changed its track, instead of passing by the Metropolitan Manila. Similarly, Typhoon Mekkhala's intense rainfall occurred along the eastern coasts, before it started to dissipate. Evidently, due to these factors the isotope values associated with those TCs were not as negative as during Rammasun. Therefore, a TC which is relatively far away from the sampling site produces an isotope signal that is not as clear and as negative, thus averaging out between the other low values from rain systems unassociated with TC.

397

4.2 Drivers of isotopic variation at Metropolitan Manila

399

As presented in section 3.1, the isotopic parameters ($\delta^{18}\text{O}$, $\delta^2\text{H}$, d-excess) show seasonal variabilities and are influenced by several climatic factors (precipitation amount, temperature and relative humidity). The scale of influence varies depending on daily or monthly values. The results indicate that $\delta^{18}\text{O}$ on daily levels is not influenced by temperature, relative humidity or precipitation amount (Fig. 2) as drivers of isotopic variability. Instead, we speculate that other processes, such as large scale convection and processes at the moisture source region might influence stable isotopes of precipitation at our study site (Conroy et al., 2016; He et al., 2018; Kurita, 2013). Interestingly, $\delta^{18}\text{O}$ is not affected by precipitation amount on short timescales (Fig. 4), which has also been previously confirmed in other tropical regions, suggesting that the tropical amount effect is not reflected on daily timescales (Belgaman et al., 2016; Dansgaard, 1964; He et al., 2018; Kurita et al., 2009; Marryanna et al., 2017; Permana et al., 2016). However, comparing monthly $\delta^{18}\text{O}$ to $\delta^2\text{H}$ and d-excess and to monthly average precipitation, relative humidity and temperature, the results are clearly different (Table 2). These monthly observations show close relationships with each other, especially $\delta^{18}\text{O}$ and precipitation amount are closely linked. The close relationship between these two parameters can be attributed to the tropical amount effect (Aggarwal et al., 2012;

416 Bowen, 2008; Conroy et al., 2016). The close relationship with $r=-0.77$ between monthly $\delta^{18}\text{O}$
417 and monthly precipitation might be likely due to the influence of regional convective activities
418 on the isotopic composition of precipitation (Bony et al., 2008; He et al., 2018; Moerman et al.,
419 2013; Risi et al., 2008).

420

421 **4.3 Distance of TCs from Metropolitan Manila**

422

423 Our observations provide details on spatial distance from collection site towards TCs' centers,
424 as our findings indicate that the distance from the storm center to the sampling site impacts
425 the isotopic value. The TCs' distance of up to 500 km to sampling site and the precipitation
426 isotope value are correlated with $r=0.55$ ($n=16$, $p\text{-value}=<0.05$ and 99% confidence level). This
427 relationship weakens with an increase in the distance from the sampling site: a distance of
428 500 to 1000 km yields an r of 0.2 ($n=19$, $p\text{-value}=0.41$), the distance of 1000 to 1500 km yields
429 an r of 0.18 ($n=24$, $p\text{-value}=0.40$), while a 1500 to 2000 km distance results in an r of 0.1 ($n=21$,
430 $p\text{-value}=0.69$). This suggests that a TC more than 500 km away from the sampling site has no
431 influence on precipitation isotopes (Munksgaard et al., 2015). Thus, the closer the TC is to the
432 sampling site, the more negative the isotope signal and the larger the δ -change. This
433 relationship might provide information on storm structure and intensity, as the intensity
434 increases with proximity of the TC to the sampling location. We thus confirm that the isotope
435 value at our location is a function of the closest approach of the storm's center to the
436 sampling site (Lawrence and Gedzelman, 1996).

437

438 Figure 8 displays all the precipitation samples associated with TC presence and activities
439 within a 2000 km radius from Metropolitan Manila, and further highlights the relationship
440 between distance and isotopic depletion, additionally providing a spatial indication of TC's
441 quadrants and their tracks relative to the location of the sampling site. Strongest depletion
442 occurs within the 500 km radius. However, two relatively negative outliers are located within
443 a 1000 to 1500 km radius in the northwest quadrant (see points a and b in Fig. 9). These two
444 samples were taken during the passage of tropical storm Kujira on 22nd and 23rd of June 2015
445 (Fig. 5), which was more than 1000 km away from Metropolitan Manila travelling east along
446 the coast of Vietnam as seen with IBTrACKS data. We investigated these two samples with
447 IMERG satellite precipitation data and identified them as a part of a mesoscale system, with

448 strong convective cells delivering intense rainfall, leading to distinct isotopic depletion and
449 inducing a “false non-TC signal” of very negative $\delta^{18}\text{O}$ which is not related to TC activity.

450

451 **4.4 Cyclone track’s rainfall intensity**

452

453 IMERG satellite precipitation data also identify that the highest rainfall intensities occur at the
454 left side of the TC track for all the TC within the 500 km radius, except for Hagupit and
455 Mekkhala, which are more complex cases (Fig. 6a, b, supplementary S 2). This is in contrast
456 to the results from Villarini et al. (2011), stating that the largest rainfall accumulation appears
457 on the right side of the hurricane tracks. They also noted that large rainfall amounts occur far
458 away from the storm’s track, which we can confirm and quantify with our observations. The
459 largest rainfall totals vary in a range of 50 to 150 km away from the storm’s center depending
460 on the TC. For Kalmaegi the intense rainfall areas are up to 150 km away from the storm’s
461 center. These areas with the highest rainfall totals should most likely coincide with the most
462 negative isotope value, indicating that the strongest depletion occurs in the outer cyclonic
463 rain bands. This is consistent with previous findings (Gedzelman et al., 2003; Lawrence and
464 Gedzelman, 1996; Munksgaard et al., 2015). However, Fudeyasu et al. (2008) observed the
465 highest isotope values in the inner eye wall, i.e. in close proximity to the storm’s center. We
466 could not investigate this further as no TC passed by our site in a distance of about 20 km,
467 which is the size of a typical typhoon’s eye (Weatherford and Gray, 1988).

468

469 **4.5 Implications for paleoclimate studies**

470

471 Isotope proxies from paleoarchives such as tree rings and speleothems have been utilized to
472 reconstruct past cyclone activities (Frappier, 2013; Frappier et al., 2007; Miller et al., 2006;
473 Nott et al., 2007). For instance, stalagmites yielded a record of weekly temporal resolution
474 with negative isotopic excursions related to TC activity (Frappier et al., 2007). Such a high
475 temporal resolution from stalagmites makes our in-situ measurements very comparable,
476 highlighting the potential to use both in conjunction. Similarly, high-resolution tree ring
477 isotope analysis identified the occurrence of Hurricane Ivan and Hurricane Frances in 2004,
478 which both resulted in the lowest observed precipitation isotope values for that year (Li et
479 al., 2011). Nevertheless, it is important to consider possible limitations at the study site that

arise in paleotempestology, such as sea level change or disruption of sedimentological records through floods or tsunamis. These need to be evaluated when comparing precipitation isotopes related to TCs with other proxy records such as speleothems and coastal deposits and when choosing the study area (Oliva et al., 2017). However, the aforementioned paleotempestology studies suffer from uncertainty regarding parameters such as TC intensity and distance to the storm's center affecting the isotope signal. With our study, we provide further information on these parameters as we hypothesize that immediate proximity of a TC results in very low $\delta^{18}\text{O}$. Therefore, we might aid with a better interpretation of paleoarchives. Moreover, these studies are limited in number and only focus on a few regions affected by TCs, such as Central America and the Southeastern USA (Frappier et al., 2007; Miller et al., 2006). However, more paleotempestology studies investigating paleoarchives related to typhoon footprints covering different regions and countries would provide a better understanding of past TC activity, ultimately resulting in better and more accurate climate reconstructions. TC projections related to climate change could also be improved, which is especially relevant for decision makers dealing with TC related impacts and damages. Our in-situ isotope measurements provide baseline data input in an understudied tropical region, providing isotopic data of TC occurrence and quantifying the isotopic depletion associated with TC activity. Further, our 19-month dataset suggests that the lowest measured isotope value at the Philippines study site is associated with TC activity, resulting in the distinct negative isotopic shift in the time series (Fig. 5). As rain out history, topography, distance of track or rainfall unassociated with TCs can induce a weak or "false non-TC signal", it is important to choose stalagmites or trees as archives based on their location, ideally covering a spatial gradient thus capturing a TC in its full size.

5. Conclusions

As presented with our dataset, a strong, high-energy TC with a track directly approaching and hitting the sampling site leads to a clear isotopic signal in a time series in the Philippines. If the TC is further away, such as more than 500 km from the site, or heavy TC rainfall occurred elsewhere prior of making landfall, the signal is not as clear and might average out between other rainfall events. Other strong convective rainfall events unassociated with TCs may result in similarly low isotope values, and we label these as a weak or "false non-TC signal".

512 Therefore, our data suggests that distance of TC to the sampling site is a key factor in
513 influencing the isotope signal and that such a spatial component needs to be considered when
514 interpreting the isotope signal. However, a longer time series isotope record would help to
515 better constrain controlling factors, such as the influence of topography on high-energy TCs.
516 To what extent mountain ranges and low elevation coastal areas shape the TC induced
517 isotope signal needs further investigation. Based on our findings we conclude that the
518 location of precipitation sample collection needs to be chosen strategically. Ideally, several
519 rainwater collection stations should be operated, covering a wide geographical range such as
520 stretching from northern Luzon to its south. If such a spatial gradient was covered, a TC would
521 likely be captured in its full size. Consequently, we aim to expand our time series spatially and
522 temporally.

523

524 Previous studies conducted in other regions found that TCs can leave detectable isotopic
525 signals of very negative $\delta^{18}\text{O}$ values in precipitation (Good et al., 2014; Munksgaard et al.,
526 2015; Xu et al., 2019). Daily precipitation isotope samples confirm the hypothesis that TC
527 activities using isotopes can also be identified in the tropical Philippines. A total of 186 daily
528 precipitation samples spanning 10 March 2014 to 27 October 2015 from Metropolitan Manila
529 were analyzed for their isotopic composition, resulting in seasonal isotopic variability and in
530 TC related isotopic signatures. The mean isotopic value for the study period is -5.29 ‰ for
531 rain events unassociated with TC, whereas the average TC induced isotope value is -10.24 ‰
532 for TCs occurring within 500 km. The lowest recorded value is -13.84 ‰, which is a δ -change
533 of almost -9 ‰ compared to the mean, and it was sampled during the closest approach of
534 Typhoon Rammasun to the National Capital Region of the Philippines. Similarly, individual TCs
535 such as the intense and costly Rammasun that struck the Philippines in July 2014 or Kalmaegi
536 left characteristic isotopic signatures. During their approach, $\delta^{18}\text{O}$ values were relatively high
537 but once they moved closer to the collection site the isotopes became more depleted
538 alongside increasing rainfall amounts. Once they moved away their remnants lead again to
539 higher values. The distance of TC center to sampling site plays a key role in determining the
540 observed isotope signals. Correlation between isotopes and distance of up to 500 km was
541 found, though this relationship significantly weakens with increasing distance. Information on
542 storm structure and intensity can be derived from the interconnectedness of distance and
543 isotopic depletion, due to the fact that strong rainfall leads to increased isotopic fractionation

544 (He et al., 2018; Tremoy et al., 2014; Xu et al., 2019). The closer the TC is to the sampling
545 location, the stronger the rainfall intensities and the more negative the $\delta^{18}\text{O}$ in precipitation.
546 Additionally, we found that the degree of convection can induce a “false non-TC signal” of
547 very low isotope values not associated with TC activity. Other factors which limit the strength
548 and clarity of the isotope signal are distance of TC towards the sampling side, rain out history,
549 TC track and topography. Our dataset is the first of such record in the Philippines and provides
550 much needed data in scarcely sampled Southeast Asia. It can be used as a baseline in
551 paleotempestology studies reconstructing past TC history, in conjunction with tree ring and
552 speleothem datasets, as our data suggest that for Metropolitan Manila the lowest measured
553 isotope value is caused by typhoon activity. A higher precipitation sampling frequency on sub-
554 daily levels at several locations would yield more detailed constraints on TC parameters such
555 as storm structure, which we aim to realize in the future.

556

557

558 **Data availability**

559

560 The underlying research data can be accessed via the supplementary document.

561

562

563 **Author Contributions**

564

565 Dominik Jackisch analyzed the data and wrote the manuscript. Bi Xuan Yeo contributed to
566 data analysis and improved the manuscript. Adam D. Switzer conceived the idea, reviewed
567 and improved the manuscript. Shaoneng He provided advice, reviewed and improved the
568 manuscript. Danica Cantarero and Fernando P. Siringan collected the precipitation samples
569 and improved the manuscript. Nathalie F. Goodkin reviewed and improved the manuscript.

570

571

572 **Competing interests**

573

574 The authors declare that they have no conflict of interest.

575

576

577 **Acknowledgments**

578

579 This study is supported by the National Research Foundation Singapore and the Singapore
580 Ministry of Education under the Research Centres of Excellence Initiative. It is Earth
581 Observatory of Singapore contribution no. 188. This study is also the part of IAEA Coordinated
582 Research Project (CRP Code: F31004) on “Stable isotopes in precipitation and palaeoclimatic
583 archives in tropical areas to improve regional hydrological and climatic impact model” with
584 IAEA Research Agreement No. 17980.

585

586

587

588

589

590

591

592

593

594

595

596

597

598

599

600

601

602

603

604

605

606

607

608 **References**

609

- 610 Aggarwal, P. K., Alduchov, O. A., Froehlich, K. O., Araguas-Araguas, L. J., Sturchio, N. C. and
611 Kurita, N.: Stable isotopes in global precipitation: A unified interpretation based on
612 atmospheric moisture residence time, *Geophys. Res. Lett.*, 39(11), 1–6,
613 doi:10.1029/2012GL051937, 2012.
- 614 Alojado, D. and Padua, D. M.: Costliest Typhoons of the Philippines (1947 - 2014), [online]
615 Available from:
616 https://www.typhoon2000.ph/stormstats/WPF_CostliestTyphoonsPhilippines_201
617 5Ed.pdf (Accessed 17 September 2019), 2015.
- 618 Belgaman, H., Ichianagi, K., Tanoue, M. and Suworman, R.: Observational Research on
619 Stable Isotopes in Precipitation over Indonesian Maritime Continent, *J. Japanese
620 Assoc. Hydrol. Sci.*, 46(1), 7–28, doi:10.4145/jahs.46.7, 2016.
- 621 Bony, S., Risi, C. and Vimeux, F.: Influence of convective processes on the isotopic
622 composition ($\delta^{18}\text{O}$ and δD) of precipitation and water vapor in the tropics: 1.
623 Radiative-convective equilibrium and Tropical Ocean-Global Atmosphere-Coupled
624 Ocean-Atmosphere Response Experiment (, *J. Geophys. Res. Atmos.*, 113(19), 1–
625 21, doi:10.1029/2008JD009942, 2008.
- 626 Bowen, G. J.: Spatial analysis of the intra-annual variation of precipitation isotope ratios
627 and its climatological corollaries, *J. Geophys. Res. Atmos.*, 113(5), 1–10,
628 doi:10.1029/2007JD009295, 2008.
- 629 Chakraborty, S., Sinha, N., Chattopadhyay, R., Sengupta, S., Mohan, P. M. and Datye, A.:
630 Atmospheric controls on the precipitation isotopes over the Andaman Islands, Bay
631 of Bengal, *Sci. Rep.*, 6, 1–11, doi:10.1038/srep19555, 2016.
- 632 Cinco, T. A., de Guzman, R. G., Hilario, F. D. and Wilson, D. M.: Long-term trends and
633 extremes in observed daily precipitation and near surface air temperature in the
634 Philippines for the period 1951-2010, *Atmos. Res.*, 145–146, 12–26,
635 doi:10.1016/j.atmosres.2014.03.025, 2014.
- 636 Cinco, T. A., de Guzman, R. G., Ortiz, A. M. D., Delfino, R. J. P., Lasco, R. D., Hilario, F. D.,
637 Juanillo, E. L., Barba, R. and Ares, E. D.: Observed trends and impacts of tropical
638 cyclones in the Philippines, *Int. J. Climatol.*, 36(14), 4638–4650,
639 doi:10.1002/joc.4659, 2016.

- 640 Conroy, J. L., Noone, D., Cobb, K. M., Moerman, J. W. and Konecky, B. L.: Paired stable
641 isotopologues in precipitation and vapor: A case study of the amount effect within
642 western tropical Pacific storms, *J. Geophys. Res.*, 121(7), 3290–3303,
643 doi:10.1002/2015JD023844, 2016.
- 644 Craig, H.: Isotopic variations in meteoric waters, *Science* (80- .), 133(3465), 1702–1703,
645 doi:10.1126/science.133.3465.1702, 1961.
- 646 Cruz, F. T., Narisma, G. T., Villafuerte, M. Q., Cheng Chua, K. U. and Olaguera, L. M.: A
647 climatological analysis of the southwest monsoon rainfall in the Philippines,
648 *Atmos. Res.*, 122, 609–616, doi:10.1016/j.atmosres.2012.06.010, 2013.
- 649 Dansgaard, W.: Stable isotopes in precipitation, *Tellus*, 16(4), 436–468,
650 doi:10.3402/tellusa.v16i4.8993, 1964.
- 651 Emanuel, K.: Increasing destructiveness of tropical cyclones over the past 30 years,
652 *Nature*, 436(7051), 686–688, doi:10.1038/nature03906, 2005.
- 653 Frappier, A. B.: Masking of interannual climate proxy signals by residual tropical cyclone
654 rainwater: Evidence and challenges for low-latitude speleothem paleoclimatology,
655 *Geochemistry, Geophys. Geosystems*, 14(9), 3632–3647, doi:10.1002/ggge.20218,
656 2013.
- 657 Frappier, A. B., Sahagian, D., Carpenter, S. J., González, L. A. and Frappier, B. R.: Stalagmite
658 stable isotope record of recent tropic cyclone events, *Geology*, 35(2), 111–114,
659 doi:10.1130/G23145A.1, 2007.
- 660 Fudeyasu, H., Ichiyanagi, K., Sugimoto, A., Yoshimura, K., Ueta, A., Yamanaka, M. D. and
661 Ozawa, K.: Isotope ratios of precipitation and water vapor observed in typhoon
662 Shanshan, *J. Geophys. Res. Atmos.*, 113(12), 1–9, doi:10.1029/2007JD009313,
663 2008.
- 664 Gedzelman, S., Lawrence, J., Gamache, J., Black, M., Hindman, E., Black, R., Dunion, J.,
665 Willoughby, H. and Zhang, X.: Probing Hurricanes with Stable Isotopes of Rain and
666 Water Vapor, *Mon. Weather Rev.*, 131(6), 1112–1127, doi:10.1175/1520-
667 0493(2003)131<1112:PHWSIO>2.0.CO;2, 2003.
- 668 Van Geldern, R. and Barth, J. A. C.: Optimization of instrument setup and post-run
669 corrections for oxygen and hydrogen stable isotope measurements of water by
670 isotope ratio infrared spectroscopy (IRIS), *Limnol. Oceanogr. Methods*, 10, 1024–
671 1036, doi:10.4319/lom.2012.10.1024, 2012.

- 672 Good, S. P., Mallia, D. V., Lin, J. C. and Bowen, G. J.: Stable isotope analysis of precipitation
673 samples obtained via crowdsourcing reveals the spatiotemporal evolution of
674 superstorm sandy, *PLoS One*, 9(3), doi:10.1371/journal.pone.0091117, 2014.
- 675 Gröning, M., Lutz, H. O., Roller-Lutz, Z., Kralik, M., Gourcy, L. and Pöltenstein, L.: A simple
676 rain collector preventing water re-evaporation dedicated for δ 18O and δ 2H
677 analysis of cumulative precipitation samples, *J. Hydrol.*, 448–449, 195–200,
678 doi:10.1016/j.jhydrol.2012.04.041, 2012.
- 679 Guan, S., Li, S., Hou, Y., Hu, P., Liu, Z. and Feng, J.: Increasing threat of landfalling
680 typhoons in the western North Pacific between 1974 and 2013, *Int. J. Appl. Earth*
681 *Obs. Geoinf.*, 68(7), 279–286, doi:10.1016/j.jag.2017.12.017, 2018.
- 682 He, S., Goodkin, N. F., Jackisch, D., Ong, M. R. and Samanta, D.: Continuous real-time
683 analysis of the isotopic composition of precipitation during tropical rain events:
684 Insights into tropical convection, *Hydrol. Process.*, 32(11), 1531–1545,
685 doi:10.1002/hyp.11520, 2018.
- 686 Huffman, G. J., Bolvin, D., Braithwaite, D., Hsu, K., Joyce, R., Kidd, C., Nelkin, E. J.,
687 Sorooshian, S., Tan, J. and Xie, P.: Algorithm Theoretical Basis Document (ATBD) of
688 Integrated Multi-satellitE Retrievals for GPM (IMERG), version 4.6, Nasa [online]
689 Available from:
690 https://pmm.nasa.gov/sites/default/files/document_files/IMERG_ATBD_V4.6.pdf
691 (Accessed 11 September 2019), 2017.
- 692 Knapp, K. R., Levinson, D. H., Kruk, M. C., Howard, J. H. and Kossin, J. P.: The International
693 Best Track Archive for Climate Stewardship (IBTrACS), *Bull. Am. Meteorol. Soc.*, 91,
694 363–376, doi:10.1007/978-90-481-3109-9_26, 2010.
- 695 Kurita, N.: Water isotopic variability in response to mesoscale convective system over the
696 tropical ocean, *J. Geophys. Res. Atmos.*, 118(18), 10376–10390,
697 doi:10.1002/jgrd.50754, 2013.
- 698 Kurita, N., Ichiyanagi, K., Matsumoto, J., Yamanaka, M. D. and Ohata, T.: The relationship
699 between the isotopic content of precipitation and the precipitation amount in
700 tropical regions, *J. Geochemical Explor.*, 102(3), 113–122,
701 doi:10.1016/j.gexplo.2009.03.002, 2009.
- 702 Lagmay, A. M. F., Agaton, R. P., Bahala, M. A. C., Briones, J. B. L. T., Cabacaba, K. M. C.,
703 Caro, C. V. C., Dasallas, L. L., Gonzalo, L. A. L., Ladiero, C. N., Lapidez, J. P., Mungcal,

- 704 M. T. F., Puno, J. V. R., Ramos, M. M. A. C., Santiago, J., Suarez, J. K. and Tablazon,
705 J. P.: Devastating storm surges of Typhoon Haiyan, Int. J. Disaster Risk Reduct., 11,
706 1–12, doi:10.1016/j.ijdrr.2014.10.006, 2015.
- 707 Lawrence, J. R.: Isotopic spikes from tropical cyclones in surface waters: Opportunities in
708 hydrology and paleoclimatology, Chem. Geol., 144(1–2), 153–160,
709 doi:10.1016/S0009-2541(97)00090-9, 1998.
- 710 Lawrence, J. R. and Gedzelman, S. D.: Low stable isotope ratios of tropical cyclone rains,
711 Geophys. Res. Lett., 23(5), 527–530, 1996.
- 712 Lawrence, J. R., Gedzelman, S. D., Gamache, J. and Black, M.: Stable isotope ratios:
713 Hurricane Olivia, J. Atmos. Chem., 41(1), 67–82, doi:10.1023/A:1013808530364,
714 2002.
- 715 Li, Z. H., Labbé, N., Driese, S. G. and Grissino-Mayer, H. D.: Micro-scale analysis of tree-
716 ring $\delta^{18}\text{O}$ and $\delta^{13}\text{C}$ on α -cellulose spline reveals high-resolution intra-annual
717 climate variability and tropical cyclone activity, Chem. Geol., 284(1–2), 138–147,
718 doi:10.1016/j.chemgeo.2011.02.015, 2011.
- 719 Marryanna, L., Kosugi, Y., Itoh, M., Noguchi, S., Takanashi, S., Katsuyama, M., Tani, M. and
720 Siti-Aisah, S.: Temporal variation in the stable isotopes in precipitation related to
721 the rainfall pattern in a tropical rainforest in Peninsular Malaysia, J. Trop. For. Sci.,
722 29(3), 349–362, doi:10.26525/jtfs2017.29.3.349362, 2017.
- 723 Mei, W., Xie, S. P., Primeau, F., McWilliams, J. C. and Pasquero, C.: Northwestern Pacific
724 typhoon intensity controlled by changes in ocean temperatures, Sci. Adv., 1(4), 1–
725 8, doi:10.1126/sciadv.1500014, 2015.
- 726 Miller, D. L., Mora, C. I., Grissino-Mayer, H. D., Mock, C. J., Uhle, M. E. and Sharp, Z.: Tree-
727 ring isotope records of tropical cyclone activity., Proc. Natl. Acad. Sci. U. S. A.,
728 103(39), 14294–14297, doi:10.1073/pnas.0606549103, 2006.
- 729 Moerman, J. W., Cobb, K. M., Adkins, J. F., Sodemann, H., Clark, B. and Tuen, A. A.: Diurnal
730 to interannual rainfall $\delta^{18}\text{O}$ variations in northern Borneo driven by regional
731 hydrology, Earth Planet. Sci. Lett., 369–370, 108–119,
732 doi:10.1016/j.epsl.2013.03.014, 2013.
- 733 Munksgaard, N. C., Zwart, C., Kurita, N., Bass, A., Nott, J. and Bird, M. I.: Stable Isotope
734 Anatomy of Tropical Cyclone Ita, North-Eastern Australia, April 2014, PLoS One,
735 10(3), 1–15, doi:10.1371/journal.pone.0119728, 2015.

- 736 NDRRMC: SitRep No. 38 re Effects of Typhoon “Pablo” (Bopha), [online] Available from:
737 http://www.ndrrmc.gov.ph/attachments/article/2245/SitRep_No_38_Effects_of_T
738 yphoon_PABLO_as_of_25DEC2012_0600H.pdf (Accessed 18 September 2019),
739 2012.
- 740 NDRRMC: Final Report re Effects of Typhoon “Glenda” (RAMMASUN), [online] Available
741 from:
742 [http://ndrrmc.gov.ph/attachments/article/1293/Effects_of_Typhoon_Glenda_\(RA](http://ndrrmc.gov.ph/attachments/article/1293/Effects_of_Typhoon_Glenda_(RA)
743 MMASUN)_Final_Report_16SEP2014.pdf (Accessed 17 September 2019), 2014.
- 744 NDRRMC: Final Report re Preparedness Measures and Effects of Typhoon “Lando” (I.N.
745 Koppu), [online] Available from:
746 http://ndrrmc.gov.ph/attachments/article/2607/FINAL_REPORT_re_Preparedness
747 _Measures_and_Effects_of_Typhoon_LANDO_KOPPU_as_of_14_-_21OCT2015.pdf
748 (Accessed 17 September 2019), 2015.
- 749 Nott, J., Haig, J., Neil, H. and Gillieson, D.: Greater frequency variability of landfalling
750 tropical cyclones at centennial compared to seasonal and decadal scales, Earth
751 Planet. Sci. Lett., 255, 367–372, doi:10.1016/j.epsl.2006.12.023, 2007.
- 752 Oliva, F., Peros, M. and Viau, A.: A review of the spatial distribution of and analytical
753 techniques used in paleotempestological studies in the western North Atlantic
754 Basin, Prog. Phys. Geogr., 41(2), 171–190, doi:10.1177/0309133316683899, 2017.
- 755 Pape, J. R., Banner, J. L., Mack, L. E., Musgrove, M. L. and Guilfoyle, A.: Controls on oxygen
756 isotope variability in precipitation and cave drip waters, central Texas, USA, J.
757 Hydrol., 385(1–4), 203–215, doi:10.1016/j.jhydrol.2010.02.021, 2010.
- 758 Park, M. S., Lee, M. I., Kim, D., Bell, M. M., Cha, D. H. and Elsberry, R. L.: Land-based
759 convection effects on formation of tropical cyclone Mekkhala (2008), Mon.
760 Weather Rev., 145(4), 1315–1337, doi:10.1175/MWR-D-16-0167.1, 2017.
- 761 Permana, D. S., Thompson, L. G. and Setyadi, G.: Journal of Geophysical Research :
762 Oceans, , 1–18, doi:10.1002/2015JC011534.Received, 2016.
- 763 Philippine Statistics Authority: Philippine Population Surpassed the 100 Million Mark
764 (Results from the 2015 Census of Population), [online] Available from:
765 <http://www.psa.gov.ph/population-and-housing/node/120080> (Accessed 15
766 September 2019), 2017.
- 767 Poméon, T., Jackisch, D. and Diekkrüger, B.: Evaluating the performance of remotely

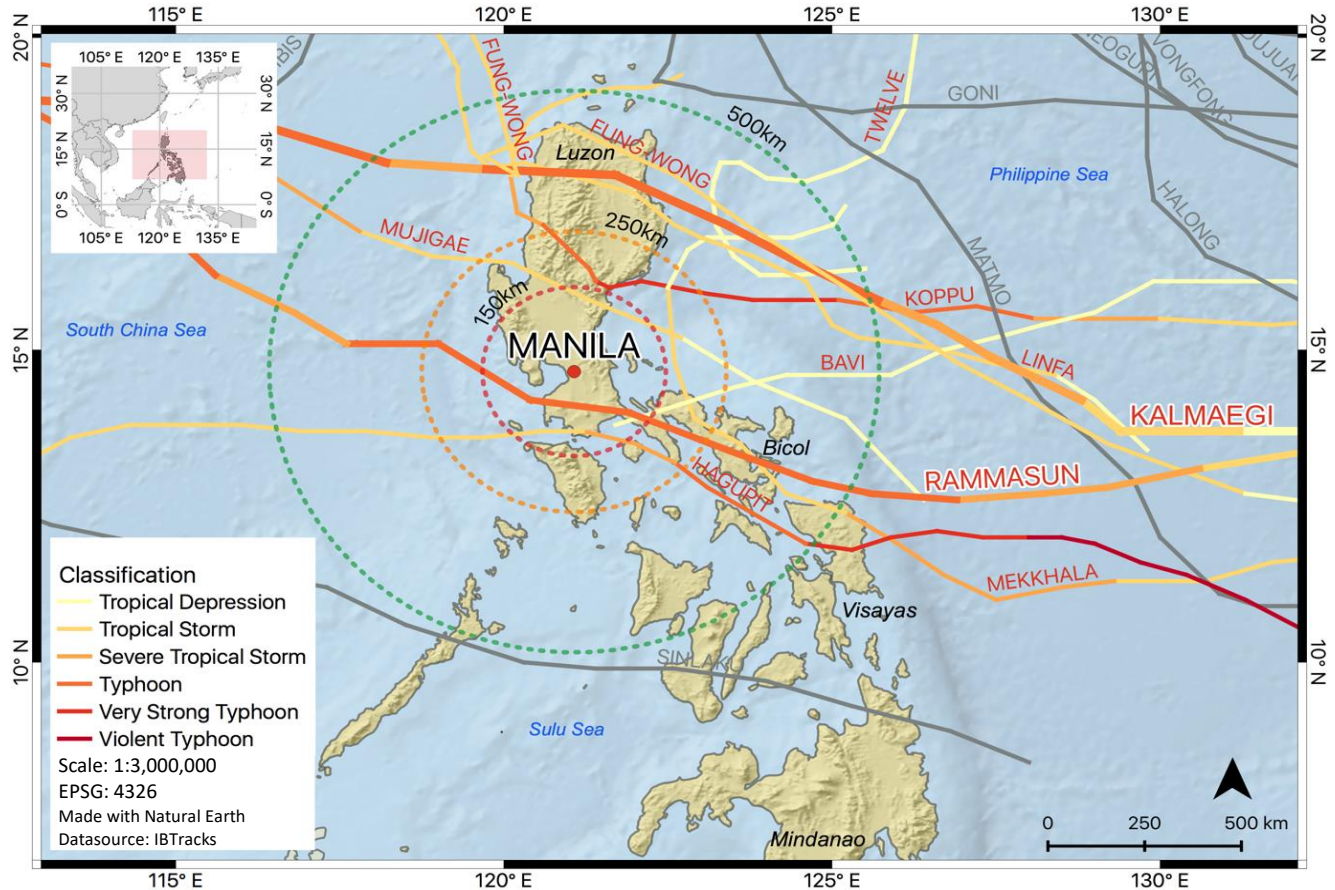
- 768 sensed and reanalysed precipitation data over West Africa using HBV light, J.
769 Hydrol., 547, doi:10.1016/j.jhydrol.2017.01.055, 2017.
- 770 Rios Gaona, M. F., Villarini, G., Zhang, W. and Vecchi, G. A.: The added value of IMERG in
771 characterizing rainfall in tropical cyclones, Atmos. Res., 209, 95–102,
772 doi:10.1016/j.atmosres.2018.03.008, 2018.
- 773 Risi, C., Bony, S., Vimeux, F., Descroix, L., Ibrahim, B., Lebreton, E., Mamadou, I. and
774 Sultan, B.: What controls the isotopic composition of the African monsoon
775 precipitation? Insights from event-based precipitation collected during the 2006
776 AMMA field campaign, Geophys. Res. Lett., 35(24), 1–6,
777 doi:10.1029/2008GL035920, 2008.
- 778 Soria, J. L. A., Switzer, A. D., Villanoy, C. L., Fritz, H. M., Bilgera, P. H. T., Cabrera, O. C.,
779 Siringan, F. P., Maria, Y. Y. S., Ramos, R. D. and Fernandez, I. Q.: Repeat storm
780 surge disasters of typhoon haiyan and its 1897 predecessor in the Philippines, Bull.
781 Am. Meteorol. Soc., 97(1), 31–48, doi:10.1175/BAMS-D-14-00245.1, 2016.
- 782 Takagi, H. and Esteban, M.: Statistics of tropical cyclone landfalls in the Philippines:
783 unusual characteristics of 2013 Typhoon Haiyan, Nat. Hazards, 80(1), 211–222,
784 doi:10.1007/s11069-015-1965-6, 2016.
- 785 Tremoy, G., Vimeux, F., Soumana, S., Souley, I. and Risi, C.: Clustering mesoscale
786 convective systems with laser-based water vapor d18O monitoring in Niamey
787 (Niger), J. Geophys. Res. Atmos. Res., 5079–5103,
788 doi:10.1002/2013JD020968. Received, 2014.
- 789 Villafuerte, M. Q., Matsumoto, J., Akasaka, I., Takahashi, H. G., Kubota, H. and Cinco, T. A.:
790 Long-term trends and variability of rainfall extremes in the Philippines, Atmos.
791 Res., 137, 1–13, doi:10.1016/j.atmosres.2013.09.021, 2014.
- 792 Villarini, G., Smith, J. A., Baeck, M. L., Marchok, T. and Vecchi, G. A.: Characterization of
793 rainfall distribution and flooding associated with U.S. landfalling tropical cyclones:
794 Analyses of Hurricanes Frances, Ivan, and Jeanne (2004), J. Geophys. Res. Atmos.,
795 116(23), 1–19, doi:10.1029/2011JD016175, 2011.
- 796 Weatherford, C. L. and Gray, W. M.: Typhoon Structure as Revealed by Aircraft
797 Reconnaissance. Part I: Data Analysis and Climatology, Mon. Weather Rev., 116(5),
798 1032–1043, doi:10.1175/1520-0493(1988)116<1032:TSARBA>2.0.CO;2, 1988.
- 799 Webster, P. J., Holland, G. J., Curry, J. A. and Chang, H.-R.: Changes in Tropical Cyclone

- 800 Number, Duration, and Intensity in a Warming Environment, *Science* (80-.),
801 309(4), 1844–1846, doi:10.1126/science.1116448, 2005.
- 802 Woodruff, J. D., Irish, J. L. and Camargo, S. J.: Coastal flooding by tropical cyclones and
803 sea-level rise, *Nature*, 504(7478), 44–52, doi:10.1038/nature12855, 2013.
- 804 Xie, B. and Zhang, F.: Impacts of typhoon track and Island topography on the heavy
805 rainfalls in Taiwan associated with Morakot (2009), *Mon. Weather Rev.*, 140(10),
806 3379–3394, doi:10.1175/MWR-D-11-00240.1, 2012.
- 807 Xu, T., Sun, X., Hong, H., Wang, X., Cui, M., Lei, G., Gao, L., Liu, J., Lone, M. A. and Jiang, X.:
808 Stable isotope ratios of typhoon rains in Fuzhou , Southeast China , during 2013 –
809 2017, *J. Hydrol.*, 570, 445–453, doi:10.1016/j.jhydrol.2019.01.017, 2019.
- 810
- 811
- 812
- 813
- 814
- 815
- 816
- 817
- 818
- 819
- 820
- 821
- 822
- 823
- 824
- 825
- 826
- 827
- 828
- 829
- 830
- 831

832 **Figures and Captions**

833

834



849 **Figure 1 Metropolitan Manila sampling site and TC tracks of 2014 and 2015 seasons.** Three different sized circles indicate the
850 distance to the sampling site with the outermost one being 500 km in radius. Cyclone tracks are color coded according to the
851 typhoon classification from Regional Specialized Meteorological Center (RSMC) Tokyo. Cyclones in gray color refer to TC outside
852 the 500 km radius.

853

854

855

856

857

858

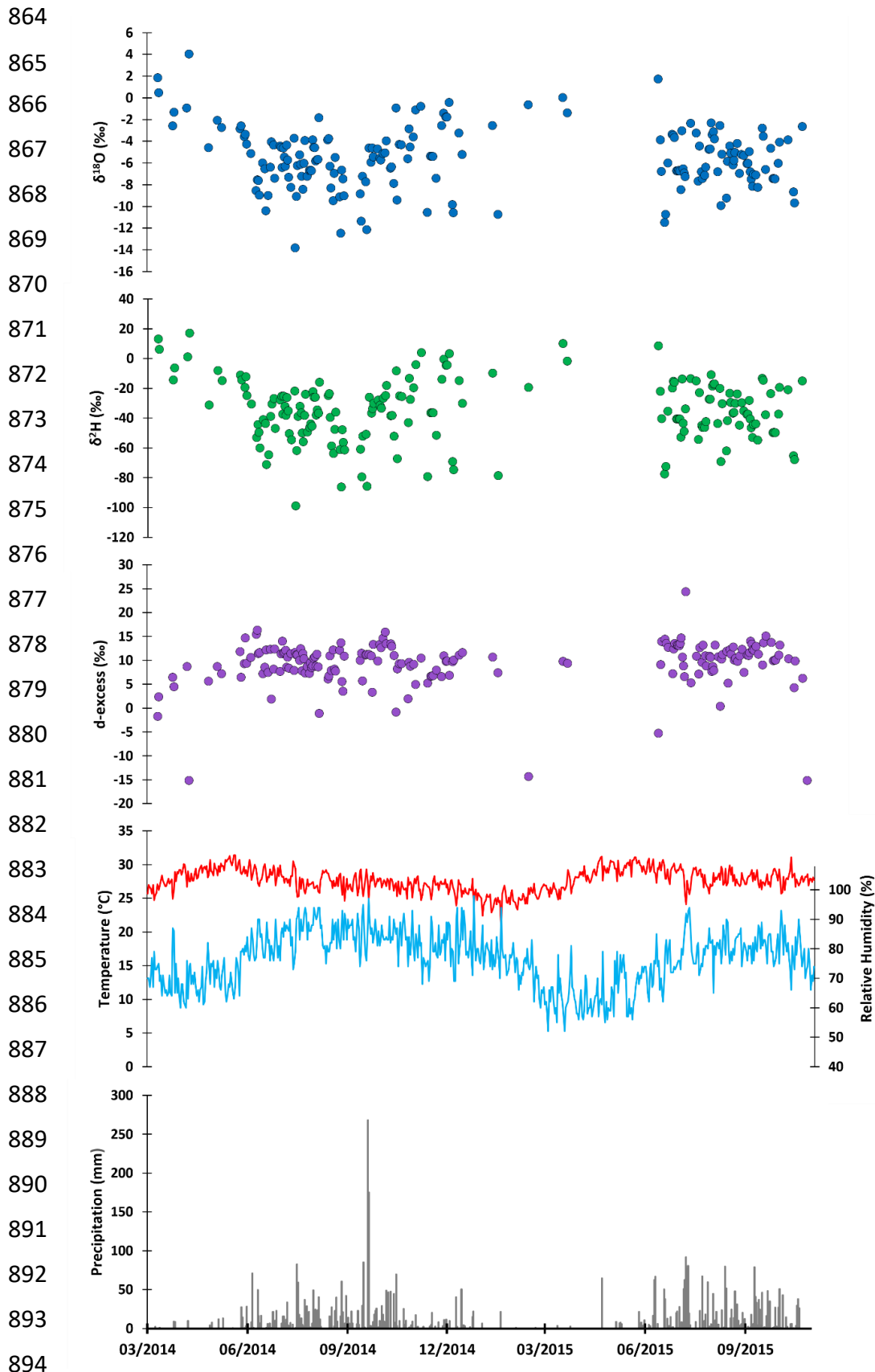
859

860

861

862

863



895 **Figure 2** Time series of daily variations of $\delta^{18}\text{O}$, $\delta^2\text{H}$, d-excess, temperature, relative humidity and precipitation amount
896 at Metropolitan Manila, Philippines.

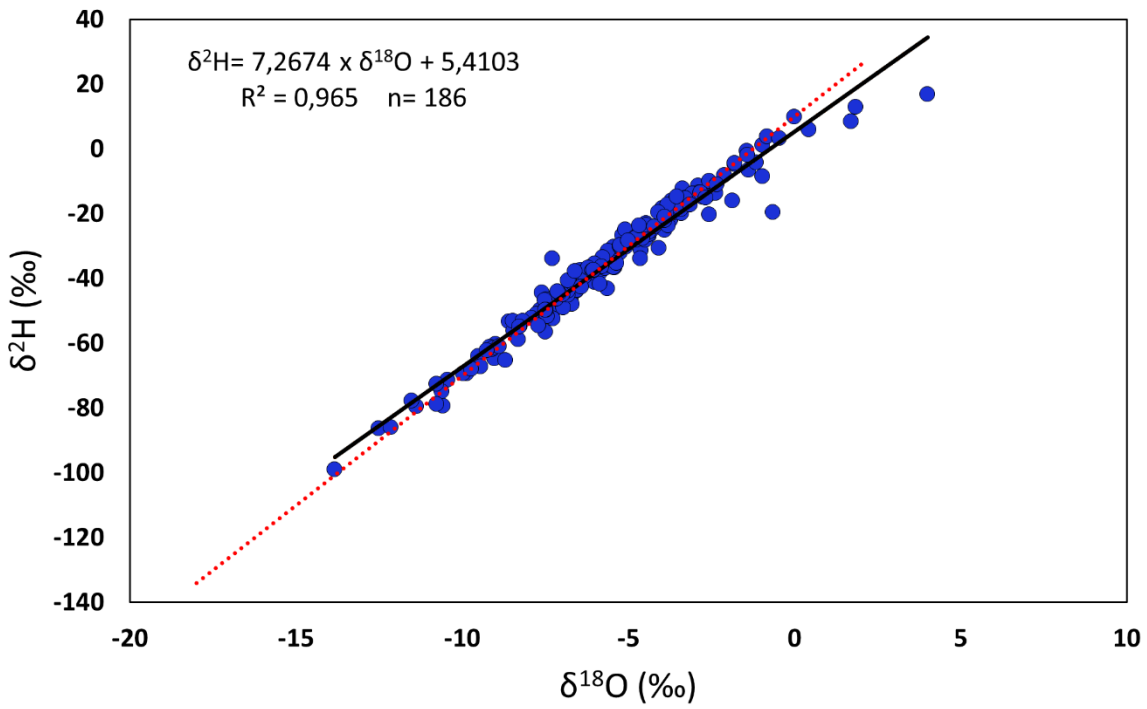


Figure 3 Local meteoric water line (LMWL) established for Metropolitan Manila, Philippines. The red dotted line represents the global meteoric water line (GMWL) ($\delta^2\text{H} = 8 \times \delta^{18}\text{O} + 10$; Craig, 1961).

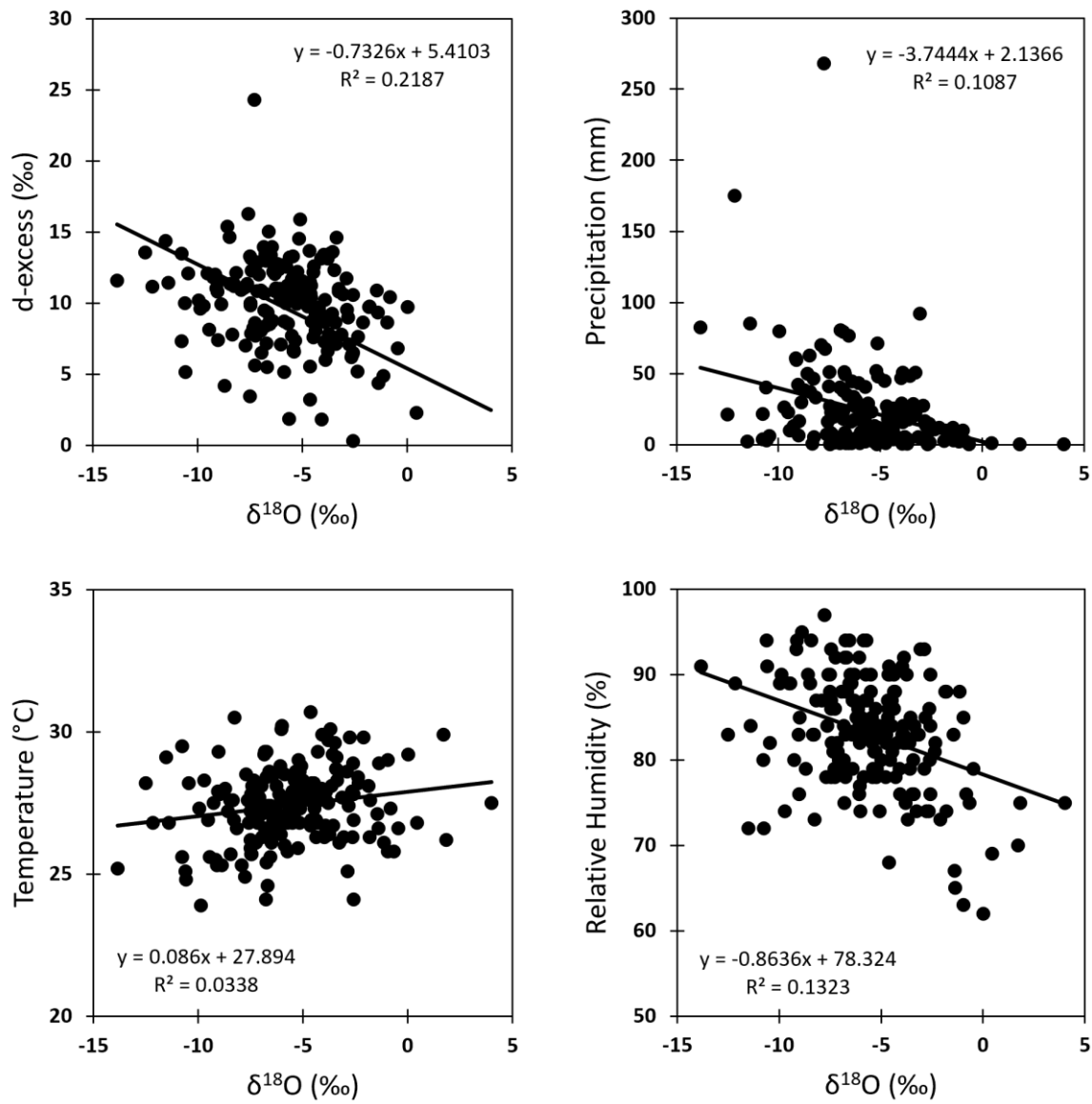


Figure 4 Correlations between daily $\delta^{18}\text{O}$ values and daily values of d-excess, precipitation amount, temperature and relative humidity. Linear regression line, correlation coefficient (R^2), slope and intercept are shown in each plot.

Metropolitan Manila daily $\delta^{18}\text{O}$ precipitation isotopes

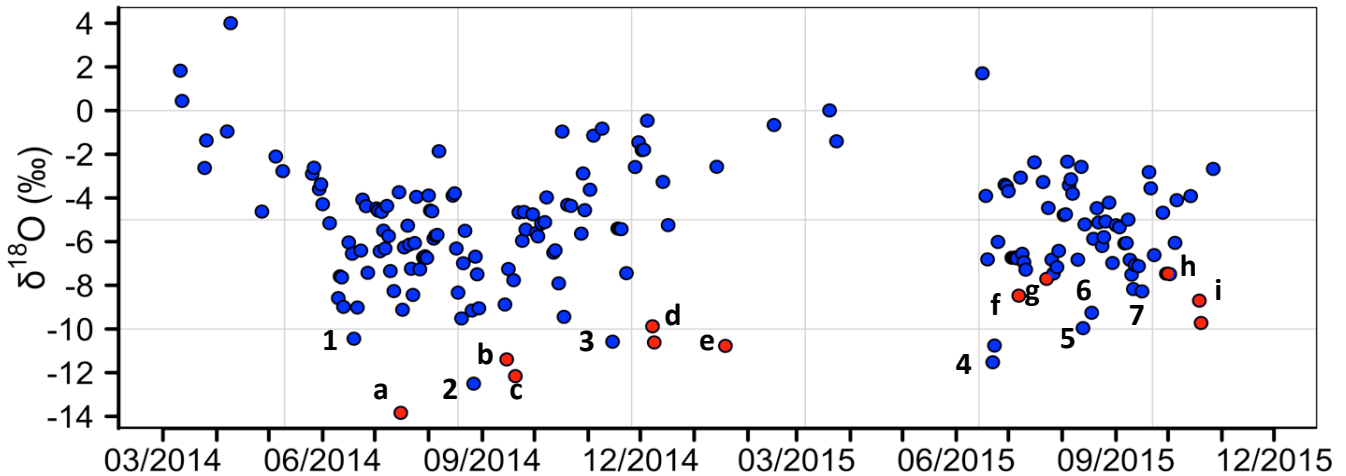


Figure 5 Complete time series of 186 precipitation samples taken between 10 March 2014 to 27 October 2015. $\delta^{18}\text{O}$ data points associated with TC activity are colored in red. Other anomalously low $\delta^{18}\text{O}$ values were investigated using IMERG satellite precipitation data. a: Rammasun 16/07/14, -13.84 ‰, 83 mm. b: Kalmaegi 15/09/14, -11.39 ‰, 85 mm. c: Fung-Wong 20/09/14, -12.16 ‰, 175 mm. d: Hagupit 8-9/12/14, -9.88 ‰, -10.62 ‰, 40 mm. e: Mekkhala 19/1/15, -10.77 ‰, 22 mm. f: Linfa 07/07/15, -8.5 ‰, 63 mm. g: Twelve 23/07/15, -7.7 ‰, 68 mm. h: Mujigae 01/10/15, -7.5 ‰, 51 mm. i: Koppu 19-20/10/15, -8.7 ‰, -9.72 ‰, 38 mm, 26 mm. 1: storm passing by 19/06/14, -10.44 ‰, 6 mm. 2: large rain areas 27/08/14, -12.5 ‰, 21 mm 3: storm passing by 15/11/14 -10.58 ‰, 3 mm. 4: large rain areas, 22-23/06/15 -10.76 ‰, -11.52 ‰, 2 mm, 4 mm. 5: heavy rainfall 13/08/15, -9.96 ‰, 80 mm. 6: heavy rainfall 18/08/15, -9.26 ‰, 13 mm. 7: local convection 16/09/15, -8.28 ‰, 47 mm.

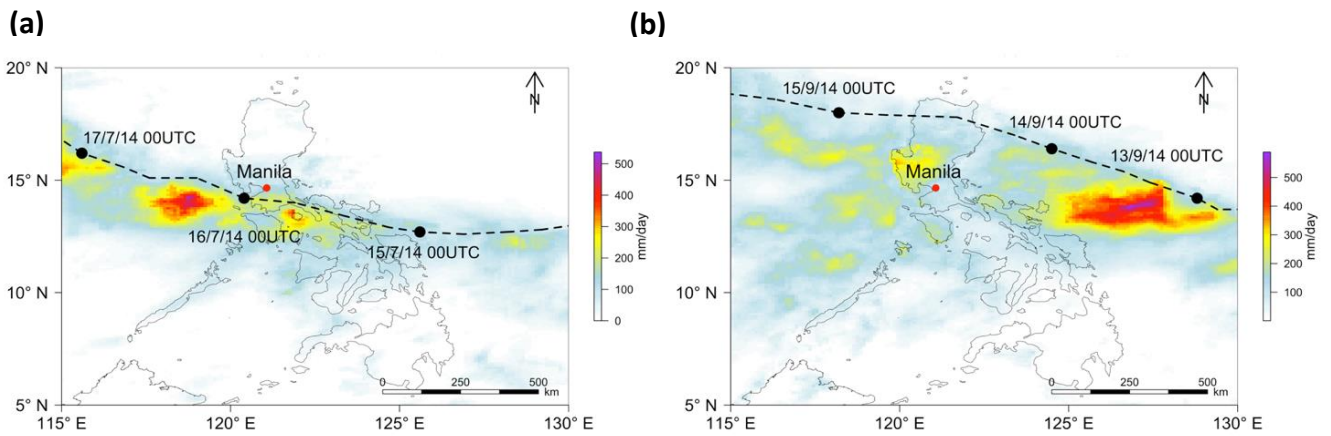


Figure 6 Accumulated precipitation from IMERG satellite data and TC tracks from IBTrACKS for a) Rammasun with precipitation accumulation for 14-17 July 2014, b) Kalmaegi with accumulated precipitation for 12-15 September 2014. Made with base layers from Natural Earth.

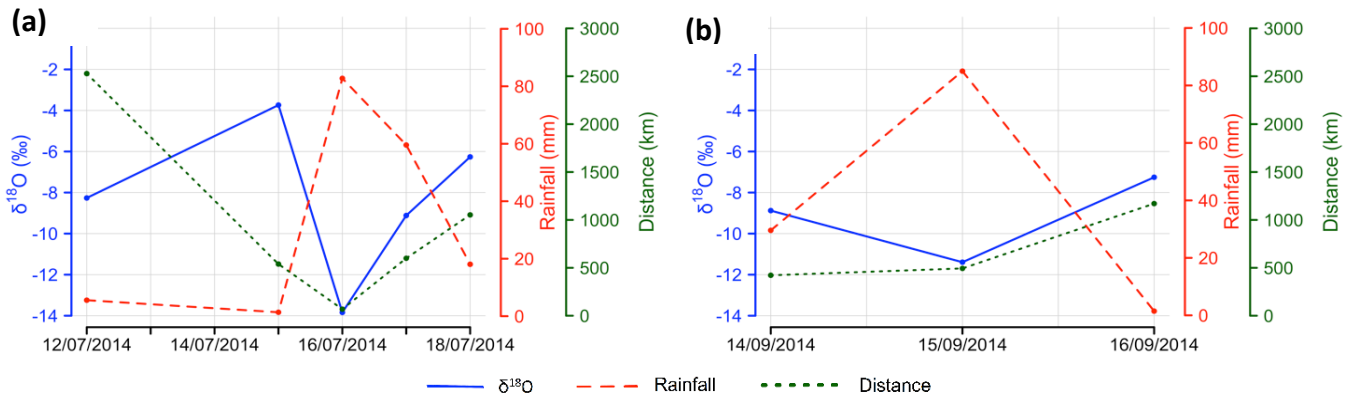


Figure 7 Isotopic signature from TCs during their passage to the Metropolitan Manila sampling site. $\delta^{18}\text{O}$ (blue color), distance from storm center to sampling location (green) and daily rainfall amount (red). a) Rammasun, b) Kalmaegi

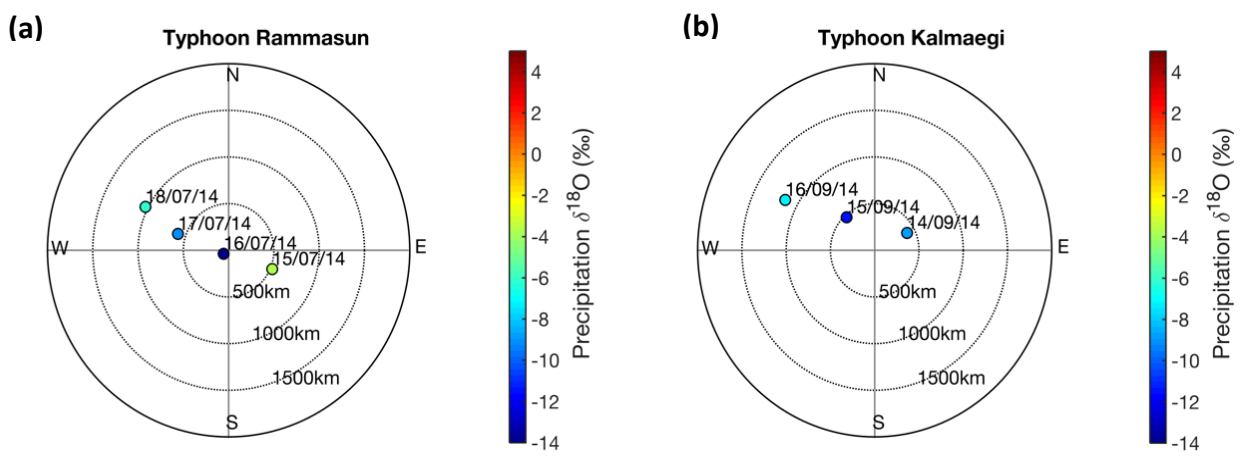


Figure 8 Spatio-temporal evolution of $\delta^{18}\text{O}$ isotopes. Centered on Metropolitan Manila collection site, different radii provide information on distance between storm's center to Metropolitan Manila. $\delta^{18}\text{O}$ values are color coded. a) Rammusun, b) Kalmaegi

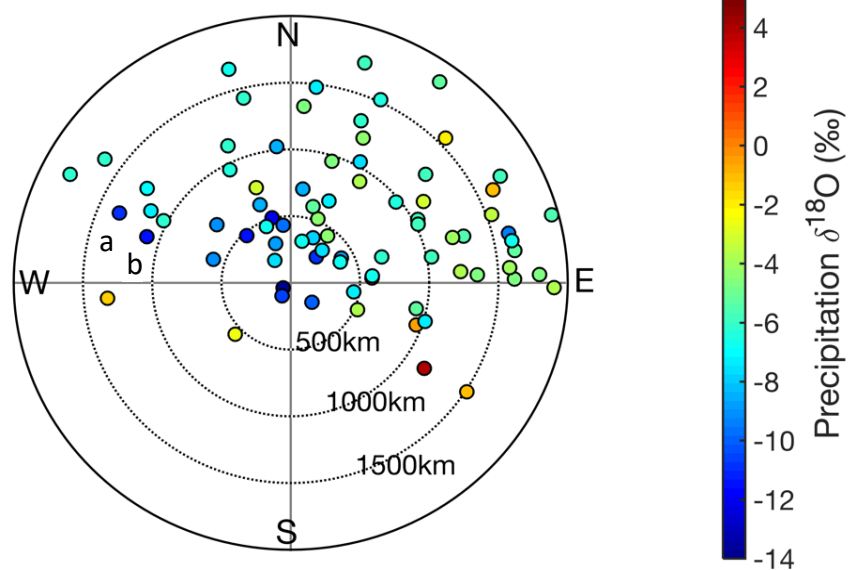


Figure 9 Spatio-temporal variation of isotopes related to TC activity within 2000 km, with different radii indicating the distance towards Metropolitan Manila. $\delta^{18}\text{O}$ values are color coded.

1057 **Tables**

1058

1059 **Table 1 Costliest typhoons in the Philippines.** Two devastating typhoons, Rammasun and Koppu (ranking 3 and 7),
 1060 occurred during our study period and made landfall. Damage in USD based on each time of TC occurrence (not adjusted to
 1061 current inflation rates).

Rank	Name (local name)	Category (Saffir-Simpson scale)	Period of occurrence	Damage in USD	Fatalities	Part of our dataset
1.	Haiyan (Yolanda)	Category 5	2-11 November 2013	~ 2.06 billion USD	~ 6000	No
2.	Bopha (Pablo)	Category 5	2-10 December 2012	~ 977 million USD	1067	No
3.	Rammasun (Glenda)	Category 5	12-17 July 2014	~ 880 million USD	106	Yes
7.	Koppu (Lando)	Category 4	12-21 October 2015	~ 310 million USD	62	Yes

References: Alojado and Padua, 2015; Lagmay et al., 2015; NDRRMC, 2012, 2014, 2015; Soria et al., 2016

1062

1063

1064

1065

1066 **Table 2 Monthly average values of the 19-month time series** of $\delta^{18}\text{O}$, $\delta^2\text{H}$, d-excess and meteorological parameters
 1067 (precipitation amount, temperature and relative humidity).

Month	$\delta^{18}\text{O}$ (\textperthousand)	$\delta^2\text{H}$ (\textperthousand)	d-excess (\textperthousand)	Precipitation (mm)	Temperature (°C)	Relative humidity (%)
Mar 14	-0.43	-0.62	2.82	4.3	27.1	70.0
Apr 14	-0.53	-4.54	-0.33	4.5	28.8	68.9
May 14	-2.89	-13.50	9.63	10.1	29.8	71.7
Jun 14	-6.90	-44.90	10.28	14.6	28.7	81.2
Jul 14	-6.46	-41.68	10.04	19.0	27.5	86.6
Aug 14	-6.39	-42.63	8.51	20.0	27.4	85.7
Sep 14	-7.29	-48.57	9.76	32.1	27.4	85.3
Oct 14	-5.24	-31.73	10.19	19.4	26.9	84.2
Nov 14	-4.39	-27.64	7.48	6.5	26.9	80.0
Dec 14	-4.72	-28.00	9.79	14.1	26.0	81.4
Jan 15	-6.67	-44.41	8.97	5.8	24.6	77.8
Feb 15	-0.66	-19.70	-14.41	0.7	25.5	70.7
Mar 15	-0.70	3.95	9.54	3.3	26.8	62.9
Apr 15				64.8	29.1	62.0
May 15				7.5	29.7	68.4
Jun 15	-5.52	-34.47	9.71	19.3	29.3	73.1
Jul 15	-6.04	-36.69	11.61	28.6	27.8	80.5
Aug 15	-5.25	-32.28	9.74	18.4	28.0	81.1
Sep 15	-6.12	-37.07	11.86	18.5	28.0	81.0
Oct 15	-6.27	-40.80	6.60	16.7	27.8	78.0

1068

1069